Korean J. Chem. Eng., 39(10), 2764-2774 (2022)
DOI: 10.1007/s11814-022-1125-0

pISSN: 0256-1115
eISSN: 1975-7220

Enhancing performance of polyacrylonitrile membranes for pervaporation dehydration of ethanol by tailoring morphology and process parameters

Seyed Mohammad Hosseini Nejad*, Amir Hossein Mostafavi*, Seyed Saeid Hosseini*,,†, Haoze Zeng***, and Lu Shao*****

*Membrane Science and Technology Research group, Department of Chemical Engineering, Tarbiat Modares University, Jalal-Ale-Ahmad, Tehran, Iran
**Institute for Nanotechnology and Water Sustainability, College of Science, Engineering and Technology, University of South Africa, Johannesburg, South Africa
***MIIT Key Laboratory of Critical Materials Technology for New Energy Conversion and Storage, State Key Laboratory of Urban Water Resource and Environment, School of Chemistry and Chemical Engineering, Harbin Institute of Technology, Harbin 150001, P. R. China
(*Received 19 November 2021 • Revised 21 March 2022 • Accepted 25 March 2022*)

Abstract−Development of high performance membranes for ethanol (EtOH) dehydration constitutes one of the main applications of pervaporation technology. In the present study, the properties of membranes derived from PAN were examined for this purpose. Heat treatment and variation of operational parameters were explored as viable strategies for enhancing the process performance. The characteristics of the membranes including morphology, thickness and sorption behavior were investigated in detail to identify their roles. Application of heat treatment with regards to polymer T_g resulted in membranes with distinct morphological and sorption characteristics. Increase in operational temperature was found effective for optimizing the opposing trends of permeate flux and separation factor. The maximum PSI value for the pristine PAN membrane was 5,564.0 $g \cdot m^{-2}h^{-1}$, which occurred for operation at 50 °C. Also, application of heat treatment led to drop in flux and increase in separation factor by which PSI reached 41.3 $kg \cdot m^{-2}h^{-1}$, which was 7.5 times than that of pristine PAN membrane. This study demonstrates successful implementation of facile strategies for tuning the characteristics and performance of membranes derived from PAN for efficient dehydration of EtOH via pervaporation process.

Keywords: Polyacrylonitrile, Pervaporation, Membrane, Ethanol Dehydration, Heat Treatment

INTRODUCTION

The growing demand for energy along with the rapid drainage of oil and gas reservoirs have motivated efforts for identification and exploration of alternative fuels. Ethanol (EtOH), as one of the environmentally friendly energy carriers, continues to gain more and more attention owing to its numerous benefits. EtOH is often accompanied by water in the mixture, especially in the course of production. Over the years, various separation methods have been explored for dehydration of EtOH mixtures. The conventional separation technologies used for this purpose suffer from major limitations, notably the presence of azeotropic point as well as high energy and operational costs especially in the case of established technologies like distillation. Therefore, alternative separation technologies with higher efficiency and less costs have been developed for EtOH dehydration [1,2].

Membrane separation processes are of particular interest thanks to the enormous advantages, such as lower energy consumption, smaller footprint, less complexity as well as lower costs compared to the rivals [3-5]. Diverse membrane materials and processes have been investigated in terms of potential for EtOH dehydration including hyperfiltration [6,7] and membrane distillation characterized by offering relatively high flux and moderate selectivity [8,9]. This also includes pervaporation process by membranes with moderate flux and high separation factor [10-14] as well as hybrid processes [15].

Pervaporation is a high-performance process with several advantages. This membrane-based technology is capable of purifying various organic and inorganic mixtures as well as hydrocarbons and plays vital role in the chemical industry [1,16-18]. For instance, recently in our group, nanocomposite pervaporation membranes were developed based on polystyrene and its derivative blends and nanocomposites for hydrazine dehydration. Hydrazine is an essential inorganic chemical with various applications, such as serving as the fuel for jets, rockets, missiles and space shuttles [19]. Also, Raza et al. separated ethyl acetate from water relying on development of organo-silica membranes. Ethyl acetate is a widely used solvent, especially for paints, varnishes, lacquers, cleaning mixtures, and perfumes [20]. Furthermore, Liu et al. optimized butanol recovery from hydrocarbon mixture in a pervaporation process and explored possible methods for optimization of the process conditions [21]. These exemplary applications clearly showcase the large potential

†To whom correspondence should be addressed.
E-mail: saeid.hosseini@modares.ac.ir

and high impact of the pervaporation process in the production of wide ranges of specialty chemicals and energy carriers.

The preferred membranes for use in pervaporation are in the form of asymmetric structure typically composed of a dense skin layer on top supported by a microporous substructure. However, the intrinsic properties of potential materials as membranes are investigated in their dense structure. Solution-diffusion is the well known governing mechanism for the transport of species in pervaporation and relies on the dissolution of the components in the membrane matrix followed by diffusion and desorption [22,23]. Separation is achieved based on the difference in the thermodynamics and kinetic of transport of different species across the membrane.

Proper selection of materials and fabrication technique play vital roles in the development of desirable morphology that could result in high performance for pervaporation separation of intended compounds. In the case of EtOH dehydration, it would be ideal to have a membrane that promotes high permeation of water as opposed to EtOH. To achieve this, the physicochemical characteristics of the membrane, such as hydrophilicity, are of great importance. The most common materials used so far for EtOH dehydration include PDMS [24], PVA [25], PSF [26], PEI [27], PA [28], PTMSP [29], and PVP/PVAc [30], CS/HEC [31] and blends of NR and PAA [32].

Polyacrylonitrile (PAN) is a thermoplastic polymer with the chemical formula of $(C_3H_3N)_n$ and exhibits hydrophilic characteristics. The membranes made of PAN typically possess good mechanical and chemical stability [33-35]. PAN is widely employed for fabrication of membranes with various applications such as nanofiltration for produced water treatment, metal recovery from electroplating wastewaters, concentration of whey or protein streams, concentration of oil/water mixtures, bacterial removal from water by microfiltration and biomedical applications among others [36-40]. Specially, due to its unique features, PAN has been widely used as the support, but not skin, layer for fabrication of pervaporation membranes for EtOH recovery [41]. All above highlight the large potential of PAN for diverse separation applications.

The most popular method for the preparation of nonporous membranes is via solution casting by which the solvent is gradually removed from the solution, which results in the formation of final membrane structure. Although membrane characteristics can be regulated before and during the phase inversion process, there exist several physical and chemical treatment methods that can be used the for tuning and alteration of the characteristics of the membrane after formation [42]. Application of thermal treatment protocols with respect to the glass transition temperature (T_g) of polymer is one of such methods that has shown a proven record of being effective in altering the microstructure of the membranes [43,44]. Often, thermal treatment is named as *annealing* if the employed temperature falls above the polymer T_g. Significant improvements were achieved in controlling the size and composition of free volumes and subsequently resistance of the membrane toward plasticization phenomena by using thermal treatment method [45]. One of the most important features of PAN membranes is its moderate T_g of around 95 °C, which makes it possible to undergo heat treatment without needing high energy.

Beside the significance of membrane material, the separation performance of a membrane is also highly dependent on the fabrication parameters and operational conditions. Operational conditions such as feed composition and temperature, flow rates, pressure and membrane surface area all play a role in the overall performance and efficiency of the process. However, the impact of each parameter largely varies depending on the nature and type of the process under investigation.

According to a literature survey, in the majority of studies devoted to the exploration of PAN as the membranes for pervaporation dehydration of EtOH, it has been used as support layer but not the active layer. On the contrary, PAN has been used as the active layer for variety of other applications but not for EtOH dehydration by pervaporation. This has led to the notion for this research to initiate development of PAN membranes and explore the characteristics for EtOH dehydration for the first time. In the present paper, pristine membranes were fabricated from PAN by knife and solution casting methods and then compared. To tune the microstructure and morphology of the resultant membranes aiming to improve the process performance, thermal treatment was applied as a simple modification tool and the effects were investigated. In addition, the operational temperature was varied to identify the optimum conditions. To the best of our knowledge, this is the first investigation on the effect of thermal treatment on the characteristics and separation performance of PAN pervaporation membranes for EtOH dehydration.

EXPERIMENTAL

1. Materials

Polyacrylonitrile (PAN, M_w=90 kDa, density=1.17 g·mL^{-1}) was purchased from Iran Polyacryl Co. (Isfahan, Iran). Dimethylformamide (DMF, density=0.944 g·mL^{-1}, vapor pressure=0.516 kPa) was purchased from Merck (Darmstadt, Germany) and used for the preparation of dope solutions. DMF was selected as the solvent due to its lower boiling point (153 °C) compared to other common solvents to facilitate faster solvent evaporation without needing much thermal energy. Furthermore, it has a closer solubility parameter to that of PAN enabling faster and easier dissolution [46]. EtOH (density=0.789 g·mL^{-1}, vapor pressure=5.92 kPa) was procured from HamounTeb Co. (Iran). Ultrapure deionized (DI) water was instantly generated in the laboratory and used for the preparation of aqueous feed solution by mixing with EtOH.

2. Membrane Preparation

First, solutions of PAN in DMF (20 wt%) were prepared by gradually adding polymer powders into the solvent and then stirring with the aid of magnetic stirrer at 60 °C for 6 hours. Subsequently, each solution was stored for 24 hours to ensure complete degassing.

Knife and solution casting methods were used for fabrication of membranes. The first method involved spreading the solution evenly on a clean glass plate using a semi-automated film applicator followed by drying inside an oven at 60 °C for 6 hours. The nascent films obtained in this method were then vacuum dried at 60 °C and 0.1 atm for another 6 hours to remove the residual solvents. The complete solvent removal was confirmed by thermogravimetric analysis (TGA) of dried samples, since no mass loss at the region close to the boiling point of MDF was noticed (Fig. 1). The formed membranes were detached from the glass plate and stored for fur-

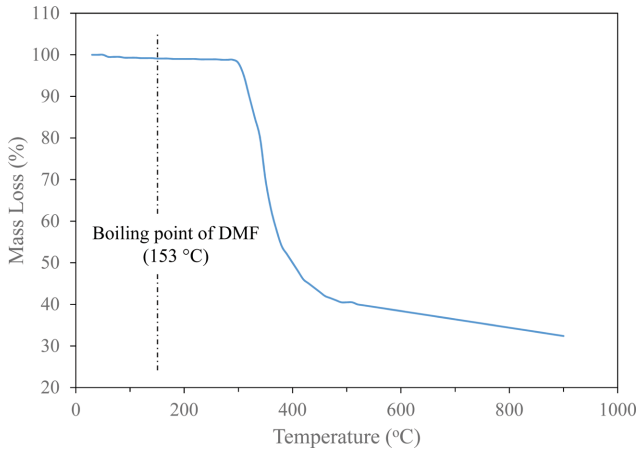

Fig. 1. TGA analysis result for pristine PAN (F1) to ensure residual solvent removal.

ther investigation.

The second method involved solution casting in a petri dish. The amount of polymer solution poured into the petri dish was calculated based on the effective surface area of petri dish, desired membrane thickness, polymer density and solution concentration in order to obtain membranes in desirable dimensions. The solution was allowed to spread evenly. It was then covered with a small, perforated piece of aluminum foil and dried in oven at 60 °C for 6 hours followed by vacuum drying at 70 °C and 0.1 atm for another 6 hours to fully remove residual solvents. The formed membranes were detached from the petri dish and stored for further investigation.

Membranes underwent thermal treatment at by heating at different temperatures including 85 °C, 100 °C and 115 °C for 12 hours. The specifications are provided in Table 1. To avoid sudden heat shocks, the oven temperature was gradually increased to the desired final temperature and also cooled naturally to the room temperature by switching the oven off.

3. Characterizations

3-1. Membrane Morphology Analysis

Developed membranes were examined carefully in terms of morphology and physical characteristics, including surface roughness, flexibility, brittleness, appearance and mechanical properties. The surface and cross-sectional microstructure of the membranes were examined using scanning electron microscopy (SEM) (ProX, Phenom, Netherland). Small pieces of membranes were immersed in liquid nitrogen and then fractured delicately with the aid of forceps. All samples were then sputtered with gold using a PVD machine (COXEM, South Korea) before observations.

Table 1. The codes and conditions of heat treatment modification applied to PAN membranes

Sample code	Parameters	
	T (°C)	t (h)
F1	-	-
F2	85	12
F3	100	12
F4	115	12

3-2. Membrane Thickness Measurement

The thickness of membranes was measured using a digital micrometer (INSIZE, 3109-25B). To ensure thickness uniformity all across the surface, different spots on each membrane sample were assessed and the average values reported.

3-3. Thermogravimetric Analysis

Thermogravimetry analysis (TGA) was carried out on a Shimadzu TGA-50H instrument. Sample in a mass of about 3 grams was loaded in the cell and heated at the rate of 10 °C·min^{-1} by purging nitrogen at flow rate of 25 mL·min^{-1}. Experiments were carried out in the range of room temperature up to 900 °C.

3-4. Membrane Sorption Measurement

Sorption tests were carried out for the analysis of the characteristics of the membranes using water and EtOH aqueous solution containing 10 wt% water. Fully dried membranes were carefully weighed before immersion in each medium. They were removed after 72 hours and drained completely using filter paper and then weighed. The amount of sorption was calculated using Eq. (1) [47, 48]:

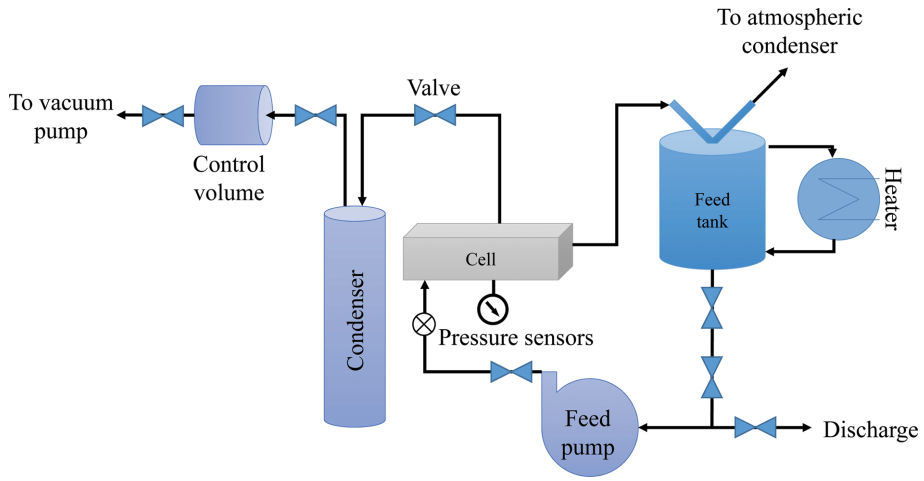

Fig. 2. Schematic diagram of the experimental set-up used for pervaporation dehydration of ethanol.

$$S = \frac{W_s - W_d}{W_d} \times 100 \quad (1)$$

where S is the amount of sorption (wt%) and W_d and W_s are weights of samples before and after sorption, respectively.

4. Pervaporation Experiments

Fig. 2 is a schematic representation of the experimental set-up used for evaluation of the separation performance of membranes. It consists of a membrane cell equipped with a feed tank and a magnetic pump for the sending feed from the tank to the cell. The feed entering cell passed over the membrane surface which was typically in the size of ~5-7 cm^2. The permeate stream was connected to a tubular trap cooled by liquid nitrogen. Sampling was carried out at different time intervals in the course of process operation for composition determination.

A series of experiments were conducted using the developed membranes F1 to F4 using EtOH solutions containing 10 wt% water as feed. The operational temperatures varied between 30 °C to 70 °C for the analysis of pristine PAN membranes and between 30 °C and 55 °C for the heat treated membranes and the effects were investigated. During each experiment, the operational temperature remained constant and the downstream pressure was set to ~0.7 mbar to provide enough driving force for permeation.

4-1. Performance Evaluation

Developed membranes were assessed in terms of performance based on few factors. The permeate flux for each component, J_i ($g \cdot m^{-2} h^{-1}$) was calculated by Eq. (2):

$$J_i = \frac{Q_i}{At} \quad (2)$$

where Q_i is the mass of collected liquid permeate of each component, A is the effective surface area of membrane and t is the operation time. The total permeate flux was the sum of individual flux of components. Separation factor (β) was calculated using Eq. (3) [14]:

$$\beta = \frac{y/(1-y)}{x/(1-x)} \quad (3)$$

where and y and x represent the fraction of water in permeate and feed streams, respectively. Also, pervaporation separation index (PSI) was calculated using Eq. (4):

$$PSI = J(\beta - 1) \quad (4)$$

where J is the permeate flux and β is the separation factor. PSI is equivalent to zero at β=1 indicating no separation occurring whatsoever.

The apparent activation energy is an indication of the magnitude of energy barrier for the permeation through the membrane. It is a complex parameter that takes into account the effect of temperature on the solubility and diffusivity of component within the membrane. To better quantify the dependence of flux to temperature, the apparent activation energy was evaluated according to the Arrhenius relationship [49]:

$$J_i = J_0 \exp\left(-\frac{E_a}{RT}\right) \quad (5)$$

where J_i is the water flux, J_0 is the pre-exponential factor, R is the gas constant, T is the absolute temperature and E_a is the apparent activation energy.

4-2. Composition Determination

To ensure accuracy of the measurements, two methods were used in tandem to evaluate the composition of permeate samples. The first method relied on the refractive index measurement using a liquid refractometer (ATAGO Abbe NAR-1T). Initially, a calibration plot was drawn based on the refractive index of a series of EtOH aqueous solutions with known concentrations. A second-degree regression was used to establish the relationship between the parameters and used for determination of the composition of the collected samples.

The second method involved measuring density of the solutions in which a predetermined volume of the EtOH aqueous solutions was weighed and then EtOH content of the solution was determined using Eqs. (6) and (7) as follows:

$$x_1 + x_2 = m \quad (6)$$

$$\frac{x_1}{\rho_1} + \frac{x_2}{\rho_2} = v \quad (7)$$

In the above equations, v is the measured volume of the sample, m is the weight of unknown sample, ρ is density and x is the weight fraction of components, and indices 1 and 2 refer to each component in the mixture, here being water and EtOH. It must be noted that the above equations are well suited for ideal solutions.

RESULTS AND DISCUSSION

1. Assessment of Casting Methods

As indicated in the experimental section, two different casting methods were used simultaneously in this study for the preparation of membranes. The aim was to explore the difference and to identify the most appropriate method. According to Tsai et al. [50], increasing the thickness of PAN membranes in pervaporation systems for separating water from EtOH resulted in increased separation index, corroborating the importance of membrane thickness and its effect on the process performance. The great advantage of knife casting method is that, due to the shear stress applied to the nascent film, the polymer chains can be oriented and this can have a great impact on the properties and performance of resultant membranes [51]. In knife casting, an adjustable film applicator was used which resulted in a series of extremely thin membranes with far smaller thickness (~10 μm) than the original gap between the applicator blade and the glass plate (200 μm). The obtained thickness was too low for withstanding the operational condition and also cumbersome for handling and sample mounting. Our observations and analysis revealed that the main culprit for the failure was the insufficient viscosity of dope solutions to maintain the integrity of fluid during the spreading. Accordingly, the solutions were overspread, resulting in membranes with thickness much lower than expected. This was coincided, considering the relatively low evaporation rate of DMF, which provided extended time for fluid relaxation during the drying stage till total solidification. Even, neither promoting the applicator gap to 400 μm, nor increasing the poly-

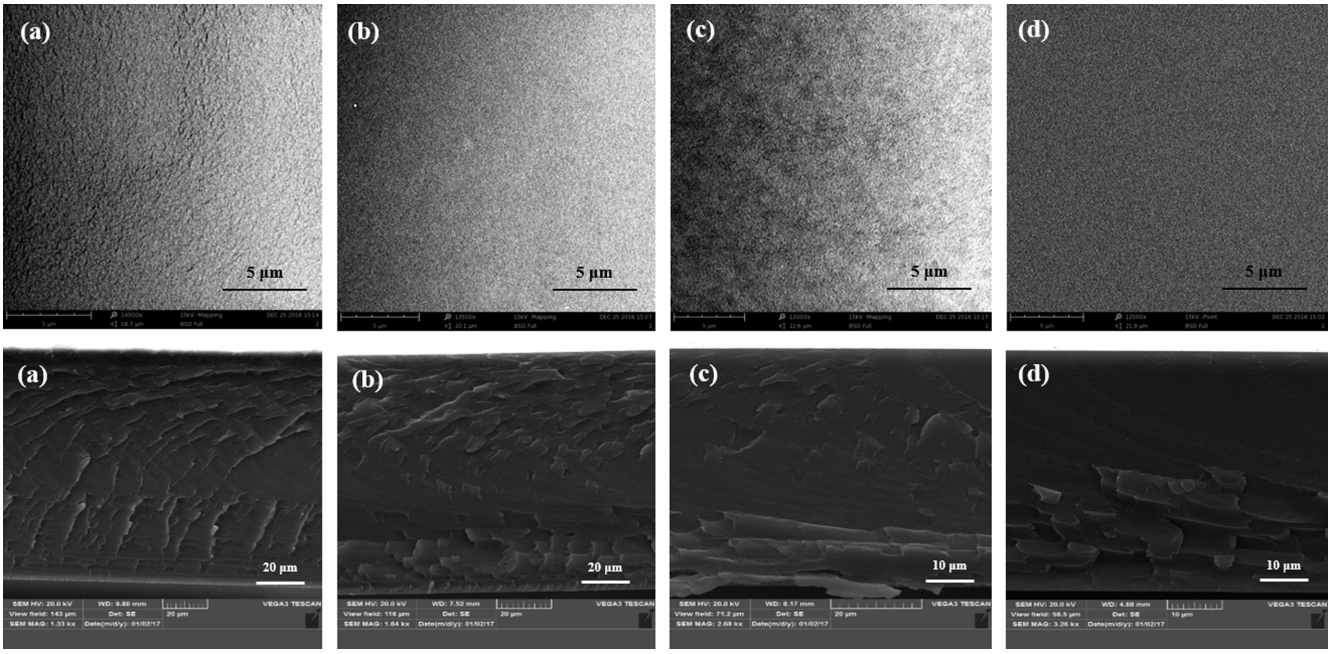

Fig. 3. Surface (upper row) and cross-sectional (lower row) SEM micrographs of pristine and heat treated PAN membranes at different temperatures: (a) Pristine PAN, (b) 85 °C, (c) 100 °C, and (d) 115 °C.

mer concentration in dope solution resulted in tangible improvements in the thickness of ultimate membranes. Despite the efforts, it was concluded that the knife casting was not an appropriate method for obtaining membranes with desired thickness.

On the other hand, by using solution casting of membranes in a petri dish, membranes with desired thickness and mechanical stability were obtained. This was actually made possible due to the confined area provided by the edges that could sustain the solution integrity. The ultimate thickness of the membranes was controlled based on the calculations on the amount of solvent loss and the left-over polymer. Therefore, all the membranes for this research were fabricated following the solution casting method. The average thickness of all the membranes was in the range of ~70±5 μm.

2. Examination of Physical Characteristics of Membranes

Based on the observations, all the membranes were transparent and exhibited limited, but yet enough, degree of flexural stability. Also, the surface of all the membranes was evenly flat. It was noted that heat treatment of membranes reduced the flexibility and imparted brittleness instead. The brittleness increased upon increase in the heat treatment temperature and duration. This was similar to the findings by Kamarudin et al., who reported that increasing the treatment temperature changed the pore structures and the tensile strength of membranes [52]. Heat treatment had no effect on the membrane thickness, samples transformed from transparent into opaque. The white color also tuned slightly into yellowish. According to the prior reports, the color change in polymeric membranes after thermal treatment can be attributed to the changes in the molecular orientation as well as the electron density for absorption of light [45]. Lastly, membranes exhibited good mechanical stability based on the observations and comparisons made before and after the pervaporation tests at different conditions.

3. Morphological Analysis of Membranes

The surface and cross-sectional SEM images demonstrating the morphology and microstructure of pristine and heat treated PAN membranes are shown in Fig. 3. Observation of the surface morphology of membranes indicated formation of a relatively rough texture with some flaws in the case of pristine PAN. However, heat treatment could obviously change the surface texture to more smooth and uniform texture. This transformation was more severe for the samples heat treated at higher temperatures of 85 °C and 115 °C. A similar trend could be seen in the transformation of the cross-sectional morphology of the membranes. While many wavy paths existed in the cross-section of pristine PAN, these patterns started to disappear gradually upon combined effects of heat treatment and rise in the treatment temperature. The morphological transformations in the microstructure of membranes are consistent with previous reports [53,54] and can be explained by focusing on the relationship between the temperature and sensitivity of polymer macromolecules with respect to T_g. In fact, heat treatment below the glass transition temperature of PAN increased the entropy of polymer chains, but this was limited only to vibrational motion. Despite its negligible effects, vibrational motions in long course of thermal treatment can lead to the possible release of free volumes and promote chain packing. The situation is completely different for the membrane heat treated at 100 °C and 115 °C which is above the T_g of PAN due to the active contributions of rotational and translational motion of polymer chains. In fact, the effect of the latter two motions is far more and incomparable to the vibrational motions and thus can bring about extensive changes to the microstructure of membranes [55,56]. Even there was almost 20 °C difference between T_g for the sample treated at 115 °C at which polymer chains experienced larger amount of rotational and translational motions, which led to the removal of extensive free volumes

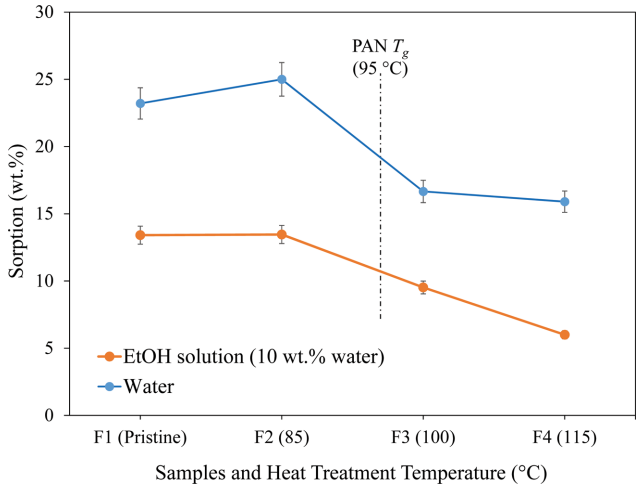

Fig. 4. Sorption properties of PAN membranes and those heat treated at different temperatures.

and release of stresses from the entire structure. Natural cooling of the sample over an extended period of time also provided enough time for the polymer chains to orient themselves in such a way that the interspaces of chains were being filled in a more ordered way during transition from high temperature to the normal state and contributed to more compaction.

4. Sorption Properties of Membranes

The governing mechanism for the transport of species in pervaporation follows the solution-diffusion theory by which the components are being sorbed into the membrane and then diffusing. The separation is achieved based on the relative rates of sorption and diffusion. Sorption is regulated by the affinity of membrane material toward each individual component and on account of its importance, it was investigated in this study to unravel its role. Fig. 4 shows the sorption results for all the membranes plotted separately for water and EtOH solution containing 10 wt% water. It can be seen that pristine PAN membrane exhibited a high water sorption capacity of ~23.2 wt%. Considering the water contact angle of 65° for PAN, this large amount of water sorption can be attributed mainly to its hydrophilicity by the presence of carbonyl functional groups with affinity toward the water molecules [57]. However, the sorption capacity of the same sample toward the EtOH solution was only ~13.4 wt%. Since the EtOH solution was composed of 10 wt% water, it is likely that a major portion of this sorption was contributed by water than by EtOH.

Heat treatment of the membranes at 85 °C led to increase in the water sorption, though increase in sorption of EtOH solution was negligible. However, the trend reversed and sorption values started to decline for the membranes heat treated at 100 °C and 115 °C and reached to 16.6 wt% and 15.9 wt% in the case of water. A similar declining effect was seen with regards to the EtOH solution. The amount of sorption was further lower for the sample treated at 115 °C. Accordingly, the least EtOH sorption value of 6.0 wt% was recorded for sample F4.

These findings correspond well with the morphological observations and can be explained using the same concept. Drop in the sorption capacity of the membranes at temperatures above the glass transition temperature can be ascribed to the rearrangement of the polymer chains due to the rotational and translational motion of polymer chains and their relaxation during cooling that led to the loss of large degree of free volumes. In fact, free volumes are the key active sites for the sorption of molecules and reduction in their population translates directly to the sorption loss. The higher the temperature, the more compact was the microstructure of the modified membrane [58,59]. From another aspect, the essential step for the penetration of molecules into the structure of membranes is the swelling phenomenon. Basically, there is a much larger energy barrier for a more compact structure to undergo swelling than a loose structure. Swelling worked effectively in the case of heat treated membranes at below T_g since the vibrational motions enhanced the amount and size of free volumes and thus water sorption was

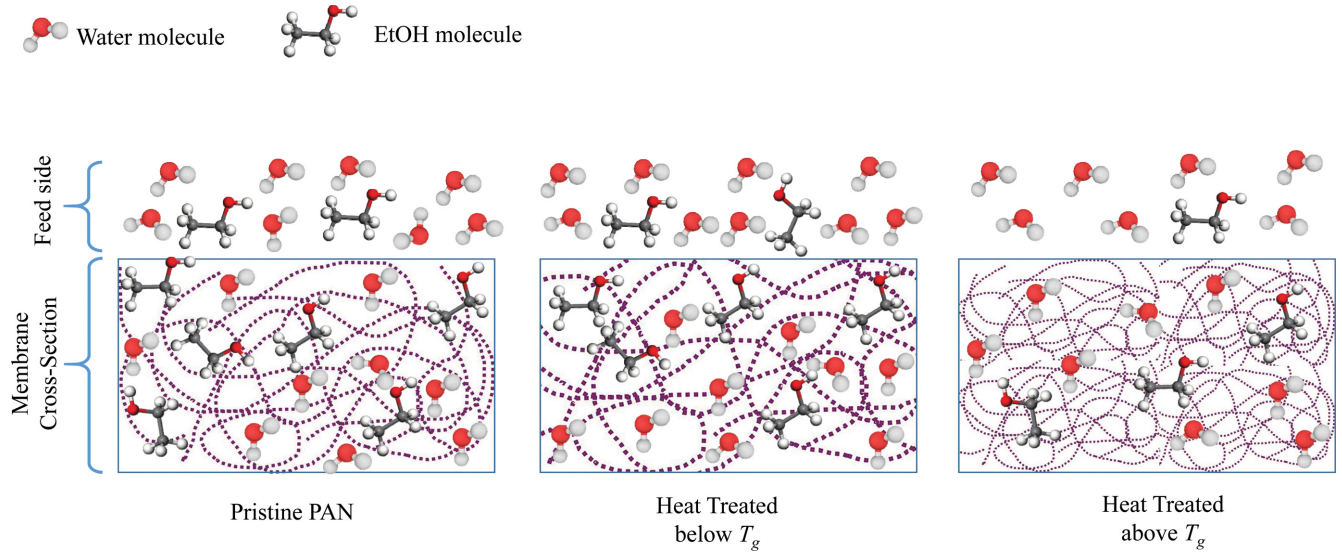

Fig. 5. Schematic representation of the sorption of pristine and heat treated PAN membranes toward water and EtOH governed by the size of molecules as well as the population and state of free volumes within different membrane structures.

increased. Though the changes were not enough to change the sorption of EtOH, considering the times a larger size of EtOH compared to that of water molecules. This was well in contrast to the case of heat treated sample above T_g for which the swelling of the matrix as a key prerequisite for sorption was hampered by the high degree of chain packing and well ordered polymer entanglements.

The overall important finding is that the sorption of all membranes toward water molecules was considerably larger than that of EtOH, which is very advantageous for the separation performance of the membranes for this application by preferential transport of water molecules that those of EtOH. Fig. 5 provides a schematic representation of this concept. These combined parameters resulted in the occurrence of a large difference between the sorption values of sample F4 toward water and EtOH. Further details are discussed in the next sections.

5. Performance of Pristine PAN Membranes and the Effect of Operational Temperature

Separation performance was first evaluated in the case of pristine PAN membranes. The feed flow rate was set to 8 L·min^{-1} and the operational temperature varied between 30 °C to 70 °C. Fig. 6 shows the trend of changes in permeate flux and separation factor at different operational temperatures. The obtained values for the permeate flux and separation factor were 522 g·m^{-2}h^{-1} and 8.6, respectively, for operation at 30 °C. Upon increase in operational temperature to 50 °C, the permeate flux increased by about 60%. But an exponential improvement in flux was noted upon further increase in operational temperature and reached to the maximum value of 3,579 g·m^{-2}h^{-1} at 70 °C. This is almost seven times of operation at 30 °C. On the other hand by following an opposite trend, the separation factor declined upon increase in operational temperature and reached to as low as 2.25 at 70 °C.

The important conclusion from the findings is the presence of an inverse relationship between the two crucial parameters of flux and separation factor. This enables deliberate selection of operational temperature depending on process requirements. The rise in permeate flux can mainly be attributed to the accelerated driving force for permeation since the vapor pressure of species are essentially elevated at higher temperatures [60]. For instance, the vapor pressure of water at 70 °C (310.6 mbar) is almost 7.3 times than that at 30 °C (42.4 mbar). In addition, the flux in pervaporation relies on the transport of molecules in their vapor phase than in their liquid form, which requires less energy to take place, especially considering the vacuum applied at the downstream. Another aspect that needs to be taken into account is that in a steady state process, the temperature of membrane matrix is equilibrated with the feed after few minutes of operation. At a higher temperature, the thermal motion and entropic activity of macromolecules present within the membrane matrix are adjusted and this facilitates the transport of species by both sorption and diffusion due to the presence of the larger free volumes aided by enhanced swelling [61,62]. Consequently, more EtOH molecules find the opportunity to permeate along with the water molecules which leads to the drop in separation factor.

Besides the role of hydrophilicity, higher sorption of water molecules, as well as diffusion due to its smaller size, the preferential and selective transport of water molecules compared to EtOH can be explained by the analysis of the activation energy of water (21.5 kJ·mol^{-1}) and EtOH (48.8 kJ·mol^{-1}). These values were calculated from the plot of ln J versus 1/T as shown in Fig. 7 and indicate

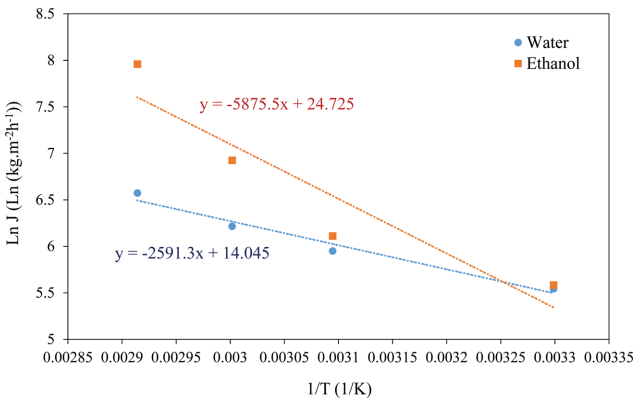

Fig. 7. The Arrhenius plot on dependence of water and ethanol flux versus temperature.

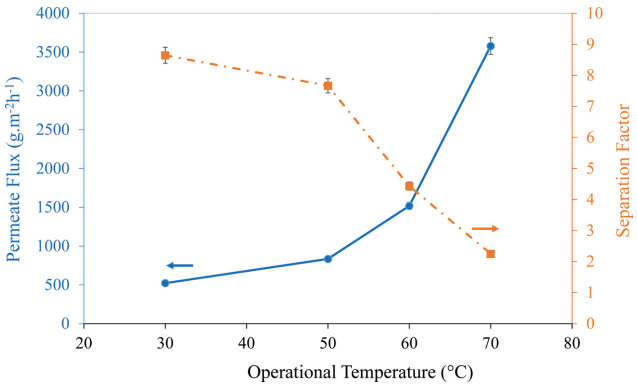

Fig. 6. Flux and separation factor for the pristine PAN membrane (F1) at different operational temperatures (Feed: EtOH solution containing 10 wt% water).

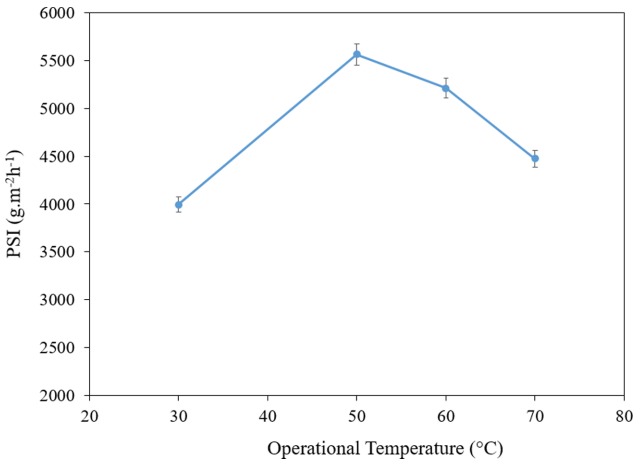

Fig. 8. PSI for the pristine PAN membrane (F1) at different operational temperatures (Feed: EtOH solution containing 10 wt% water).

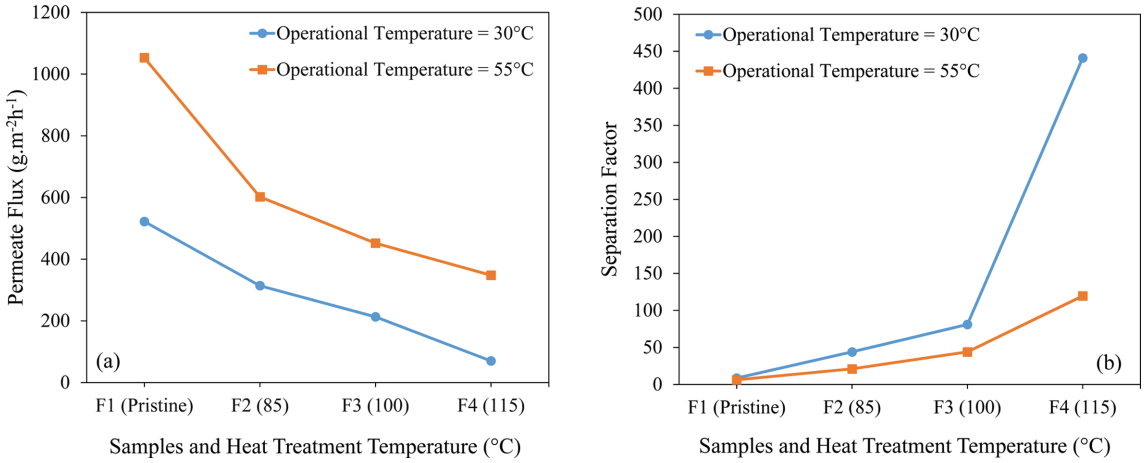

Fig. 9. Changes in (a) flux and (b) separation factor for the heat treated PAN membranes at different operational temperatures (Feed: Ethanol aqueous solution containing 10 wt water).

that the energy required for the transport of water molecules is less than that of EtOH. It should be highlighted that although the trend observed in separation factor is in good agreement with observations in other studies, some exceptions have also been reported [61-63]. This signifies the interplay of other factors, such as membrane material, that should be taken into account.

To gain insight over the overall performance of membranes, PSI values reflecting the integrated contributions of flux and separation factor were calculated and plotted in Fig. 8. It can be seen that PSI first increased and then decreased upon increase in the operational temperature. The maximum PSI belonged to operation at 50 °C with the value of 5,564.0 $g{\cdot}m^{-2}h^{-1}$, which represents the optimum condition in terms for separation performance for EtOH dehydration.

6. Performance of Heat Treated Membranes and the Effect of Treatment and Operational Temperatures

Performance of heat treated membranes was investigated at two different operational temperatures of 30 °C and 55 °C. Similar to the pristine membranes, the feed flow rate was set to 8 $L{\cdot}min^{-1}$. Fig. 9(a) shows the trend of changes in permeate flux and separation factor for the investigated membranes. Considering operation at 30 °C, while the permeate flux for the pristine PAN membranes was 522 $g{\cdot}m^{-2}h^{-1}$, application of heat treatment led to reduction in the permeate flux. The higher the heat treatment temperature, the lower the permeate flux of the resultant membrane was following the order of F4<F3<F2<F1. Accordingly, the permeate flux for the sample heat treated at 115 °C (F4) was as low as 70 $g{\cdot}m^{-2}h^{-1}$. A similar trend was observed for operation at 55 °C though the permeate flux was essentially higher than that of 30 °C. As explained previously, decline in the flux can be attributed to the more compact chain packing and presence of less free volumes in the structure of heat treated samples. In a good agreement with sorption results, the effect of compaction was stronger in heat treated at higher temperature and this hampered the transport of species through the membrane.

An interesting point was that the drop in permeate flux upon heat treatment for operation at 55 °C was less than that of operation at 30 °C. Permeate flux for the sample heat treated at 115 °C (F4) was 348 $g{\cdot}m^{-2}h^{-1}$, which is only three times less than that of pristine PAN membrane, whereas this drop was ~7.5 times for operation at 30 °C. This translates to the fact that the diminishing effect of heat treatment could be compensated, to a large extent, by adjusting the operational temperature to a higher value. This may be related to the increased motion of polymer chains that could enhance the sorption and overcome the energy barrier for the transport of species. This is well supported by other investigations [53, 54,64].

Fig. 9(b) shows the effect of heat treatment on the separation factor of membranes. As anticipated, application of heat treatment was effective in improving the separation factor of membranes. Interestingly, the extent of changes was beyond expectation and increased considerably for the heat treated sample at 115 °C (F4) for both operational temperatures. Although the impact was higher for operation at 55 °C and led to the maximum separation factor of 441.0 among all the membranes, the corresponding value for the same membrane operated at 30 °C was only 119.5. This is again

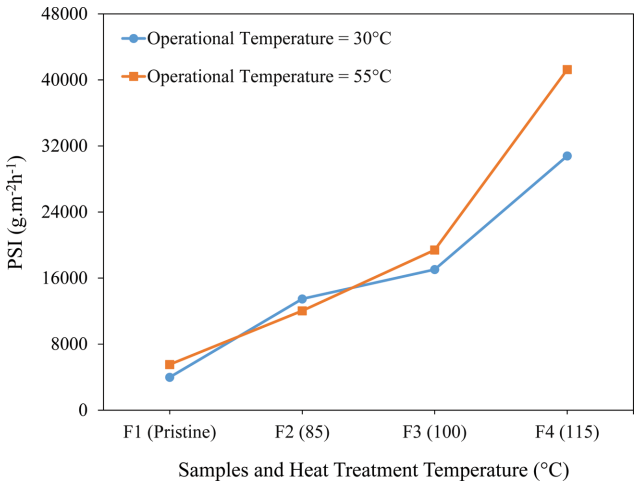

Fig. 10. Changes in PSI for the heat treated PAN membranes at different operational temperatures (Feed: EtOH solution containing 10 wt% water).

Table 2. Comparison between the characteristics and performance of different membranes used for pervaporation dehydration of EtOH

Membrane type	Water content in feed (wt%)	Feed temperature (°C)	Flux ($g \cdot m^{-2}h^{-1}$)	Separation factor	Ref.
PVA/H-ZSM5	15	30	180	46	[66]
PVA/ZIF-8-NH_2	15	45	160	148	[67]
PVA/CF-TSA	30	50	130	775	[68]
CS/siloxane	10	25	470	2,182	[69]
PVA	7	37	96	152	[70]
Heat treated PAN (F4)	10	30	70	441.0	Present study
Heat treated PAN (F4)	10	55	348	119.5	Present study

Abbreviations: PVA: Polyvinyl alcohol; CA: Cellulose acetate; GA: Glutaraldehyde; PAN: Polyacrylonitrile; PVP: Polyvinylpyrrolidone

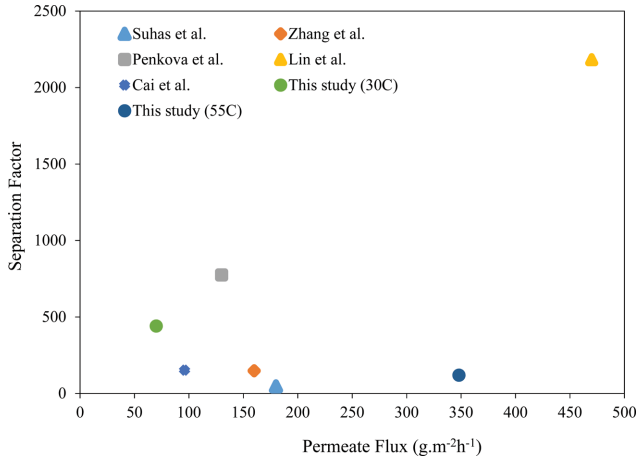

Fig. 11. Performance comparison of the developed membranes in the present study and other results published in literature for pervaporation dehydration of EtOH.

a consequence of the formation of tighter structure in the membranes upon heat treatment by providing a more controlled and selective transport based on solution-diffusion mechanism [50,65].

Another interesting consequence of heat treatment on the performance was seen in PSI trends. As shown in Fig. 10, the competing effect of flux and separation factor ended up in an eventual increase in PSI upon application of heat treatment. The effect was further extended by increase in the treatment temperature. The highest PSI was recorded for sample F4 with values of 30.8 $kg \cdot m^{-2}h^{-1}$ and 41.3 $kg \cdot m^{-2}h^{-1}$ for operations at 30 °C and 55 °C, respectively. These values were 5.6 and 7.5 times larger that than of pristine PAN membrane, respectively. These results further confirmed the successful implementation of adopted strategies of combining heat treatment and operational temperatures as an effective means for enhancing the properties and performance of developed membranes for efficient EtOH dehydration. Table 2 and Fig. 11 show the significance and state of performance for the developed membranes in the present study with respect to the comparable membranes available in the literature [66-70].

CONCLUSIONS

Membranes were developed from PAN for pervaporation dehydration of EtOH. Knife casting was not effective for membrane fabrication, but solution casting worked well and offered defect-free membranes with desirable thickness and morphology. Heat treatment of membranes with respect to T_g and variation in operational temperature were examined as potential strategies for enhancing the properties and performance of membranes. Both surface and cross sectional morphologies of membranes were affected upon heat treatment. Despite slight increase in water sorption of membranes heat treated at 85 °C, almost no change was noted in their sorption toward EtOH. On the other hand, heat treatment above T_g led to drop in sorption of membranes toward both components. The higher the treatment temperature, the larger was the drop in sorption. This was explained considering formation of a more compact structure, severe chain packing as well as the effects of sorption and diffusion and by taking into account the three times larger size of EtOH molecule than that of water. It was found by examination of pristine PAN membranes that increase in operational temperature was a useful means for adjusting the permeate flux and separation factor considering their opposite trends. The maximum PSI value for the pristine PAN membrane of 5,564.0 $g \cdot m^{-2}h^{-1}$ occurred for operation at 50 °C. Also, application of heat treatment led to drop in flux and increase in separation factor. These effects were extended by further increase in heat treatment temperature. The overall effect of heat treatment was positive and led to the enhancement of PSI as high as 41.3 $kg \cdot m^{-2}h^{-1}$ for the sample heat treated at 115 °C and operated at 55 °C equivalent to 7.5 times improvement compared to the pristine PAN membrane. This study clearly demonstrates successful identification of prominent parameters and implementation of facile strategies for tuning the characteristics and performance of membranes derived from PAN for efficient dehydration of EtOH in pervaporation process.

REFERENCES

1. P. Peng, Y. Lan, L. Liang and K. Jia, *Biotechnol. Biofuels*, **14**(1), 10 (2021).
2. S. Amid, M. Aghbashlo, M. Tabatabaei, K. Karimi, A.-S. Nizami, M. Rehan, H. Hosseinzadeh-Bandbafha, M. Mojarab Soufiyan, W. Peng and S. S. Lam, *Energy Convers. Manage.*, **227**, 113637 (2021).
3. M. Heidari, S. S. Hosseini, M. Omidkhah Nasrin and A. Ghadimi, *Sep. Purif. Technol.*, **209**, 503 (2019).
4. A. Khalid, M. Aslam, M. A. Qyyum, A. Faisal, A. L. Khan, F.

Ahmed, M. Lee, J. Kim, N. Jang, I. S. Chang, A. A. Bazmi and M. Yasin, *Renew. Sustain. Energy Rev.*, **105**, 427 (2019).
5. J. A. Dehkordi, S. S. Hosseini, P. K. Kundu and N. R. Tan, *Chem. Product Process Modeling.*, **11**(1), 11 (2016).
6. S. A. Leeper and G. T. Tsao, *J. Membr. Sci.*, **30**(3), 289 (1987).
7. H. K. Min, S. A. Sung, S. Y. Lee and S. W. Lee, *Kidney Res. Clin. Pract.*, **38**(2). 196 (2019).
8. O. Gupta, S. Roy and S. Mitra, *Ind. Eng. Chem. Res.*, **58**(39), 18313 (2019).
9. M. Gryta, A. W. Morawski and M. Tomaszewska, *Catal. Today*, **56**(1), 159 (2000).
10. R. L. G. Lecaros, S.-Y. Ho, H.-A. Tsai, W.-S. Hung, C.-C. Hu, S.-H. Huang, K.-R. Lee and J.-Y. Lai, *Sep. Purif. Technol.*, **275**, 119125 (2021).
11. M. Mokarinezhad, S. S. Hosseini, A. Ghadimi and E. Asadi, *Assessment of the effect of modification of ZIF-8 nanoparticles by CTAB cationic surfactants on the performance of ZIF-8/PVA mixed matrix membranes in pervaporation dehydration of isopropanol*, Nashrieh Shimi va Mohandesi Shimi Iran (NSMSI), Accepted In Press (2022).
12. P. Grzybek, Ł. Jakubski, P. Borys, S. Kołodziej, C. Ślusarczyk, R. Turczyn and G. Dudek, *Sep. Purif. Technol.*, **281**, 119897 (2022).
13. E. Asadi, A. Ghadimi, S. S. Hosseini, B. Sadatnia, M. Rostamizadeh and A. Nadeali, *Micropor. Mesopor. Mater.*, **329**, 111539 (2022).
14. H. S. Samanta and S. K. Ray, *Sep. Purif. Technol.*, **146**, 176 (2015).
15. M. Akieh-Pirkanniemi, G. Lisak, J. Arroyo, J. Bobacka and A. Ivaska, *J. Membr. Sci.*, **511**, 76 (2016).
16. M. Tamaddondar, H. Pahlavanzadeh, S. S. Hosseini, G. Ruan and N. R. Tan, *J. Membr. Sci.*, **472**, 91 (2014).
17. L. M. Vane, *J. Chem. Technol. Biotechnol.*, **95**(3), 495 (2020).
18. H. Zeng, S. He, S. S. Hosseini, B. Zhu and L. Shao, *Adv. Membr.*, **2**, 100015 (2022).
19. S. S. Hosseini, E. Mehralian, M. H. Ekbatan and P. Li, *Korean J. Chem. Eng.*, **38**(3), 587 (2021).
20. W. Raza, Y. Jianhua, J. Wang, H. Saulat, L. Wang, J. Lu and Y. Zhang, *J. Appl. Polym. Sci.*, **138**(37), 50942 (2021).
21. L. Liu, Y. Wang, N. Wang, X. Chen, B. Li, J. Shi and X. Li, *Biochem. Eng. J.*, **173**, 108070 (2021).
22. H. Zentou, Z. Z. Abidin, R. Yunus, D. R. Awang Biak, M. Abdullah Issa and M. Yahaya Pudza, *Chem. Eng. Res. Des.*, **175**, 320 (2021).
23. S. S. Hosseini, H. Pahlavanzadeh and M. Tamadondar, *Ir. Chem. Eng. J.*, **13**, 76 (2014).
24. M. Jafarinasab, J. Barzin, H. R. Mortaheb and H. Mobedi, *Iran. Polym. J.*, **24**(12), 989 (2015).
25. B. Villagra Di Carlo and A. C. Habert, *J. Mater. Sci.*, **48**(4), 1457 (2013).
26. S.-H. Chen, R.-M. Liou, C.-L. Lai, M.-Y. Hung, M.-H. Tsai and S.-L. Huang, *Desalination*, **234**(1), 221 (2008).
27. J. Li, X. Si, X. Li, N. Wang, Q. An and S. Ji, *Sep. Purif. Technol.*, **192**, 205 (2018).
28. M. B. M. Y. Ang, S.-H. Huang, M.-W. Chang, C.-L. Lai, H.-A. Tsai, W.-S. Hung, C.-C. Hu and K.-R. Lee, *Sep. Purif. Technol.*, **235**, 116155 (2020).
29. S. Claes, P. Vandezande, S. Mullens, R. Leysen, K. De Sitter, A. Andersson, F. H. J. Maurer, H. Van den Rul, R. Peeters and M. K. Van Bael, *J. Membr. Sci.*, **351**(1-2), 160 (2010).
30. R. C. A. Amarante and A. A. Donaldson, *Sep. Purif. Technol.*, **258**, 117953 (2021).
31. M. G. Mali and G. S. Gokavi, *AIP Conf Proc.*, **1989**(1), 020027 (2018).
32. S. Amnuaypanich, T. Naowanon, W. Wongthep and P. Phinyocheep, *J. Appl. Polym. Sci.*, **124**(S1), E319 (2012).
33. H. R. Shahriari and S. S. Hosseini, *Chem. Eng. Process. - Process Intensification*, **147**, 107766 (2020).
34. Z.-G. Wang, L.-S. Wan and Z.-K. Xu, *J. Membr. Sci.*, **304**(1), 8 (2007).
35. A. A. Yushkin, M. N. Efimov, A. O. Malakhov, G. P. Karpacheva, G. Bondarenko, L. Marbelia, I. F. J. Vankelecom and A. V. Volkov, *React. Funct. Polym.*, **158**, 104793 (2021).
36. N. Scharnagl and H. Buschatz, *Desalination*, **139**(1), 191 (2001).
37. S. S. Hosseini, A. Nazif, M. A. Alaei Shahmirzadi and I. Ortiz, *Sep. Purif. Technol.*, **187**, 46 (2017).
38. X. Zhang, S. Yang, B. Yu, Q. Tan, X. Zhang and H. Cong, *Sci. Rep.*, **8**(1), 1260 (2018).
39. M. A. Alaei Shahmirzadi and S. S. Hosseini, *Ir. Chem. Eng. J.*, **13**(77), 91 (2015).
40. S. S. Hosseini, H. Khodadadi and B. Bakhshi, *Korean J. Chem. Eng.*, **38**(1), 32 (2021).
41. Y.-H. Huang, S.-H. Huang, W.-C. Chao, C.-L. Li, Y.-Y. Hsieh, W.-S. Hung, D.-J. Liaw, C.-C. Hu, K.-R. Lee and J.-Y. Lai, *Polym. Int.*, **63**(8), 1478 (2014).
42. A. H. Mostafavi, A. K. Mishra, M. Ulbricht, J. Denayer and S. S. Hosseini, *J. Membr. Sci. Res.*, **7**(4), 230 (2021).
43. Y.-J. Kim, C. H. Ahn and M. O. Choi, *Eur. Polym. J.*, **46**(10), 1957 (2010).
44. B. Liu, S. Wang, P. Zhao, H. Liang, W. Zhang and J. Crittenden, *Appl. Surf. Sci.*, **435**, 415 (2018).
45. X. Duthie, S. Kentish, S. J. Pas, A. J. Hill, C. Powell, K. Nagai, G. Stevens and G. Qiao, *J. Polym. Sci., Part B: Polym. Phys.*, **46**(18), 1879 (2008).
46. A. Hamta, F. Zokaee Ashtiani, M. Karimi and A. Safikhani, *Polym. Adv. Technol.*, **32**(2), 872 (2021).
47. B. Liang, K. Pan, L. Li, E. P. Giannelis and B. Cao, *Desalination*, **347**, 199 (2014).
48. M. A. Alaei Shahmirzadi, S. S. Hosseini, G. Ruan and N. R. Tan, *RSC Adv.*, **5**(61), 49080 (2015).
49. Y. M. Xu, S. Japip and T.-S. Chung, *J. Membr. Sci.*, **595**, 117571 (2020).
50. H. Tsai, Y. Ciou, C. Hu, K. Lee, D. Yu and J. Lai, *J. Membr. Sci.*, **255**(1-2), 33 (2005).
51. S. Alibakhshi, M. Youssefi, S. S. Hosseini and A. Zadhoush, *Polym. Eng. Sci.*, **61**(3), 742 (2021).
52. D. Kamarudin, N. Awanis Hashim, B. H. Ong, Y. Kakihana, M. Higa and H. Matsuyama, *J. Environ. Chem. Eng.*, **9**(4), 105769 (2021).
53. A. Rahimpour, S. S. Madaeni, M. Amirinejad, Y. Mansourpanah and S. Zereshki, *J. Membr. Sci.*, **330**(1-2), 189 (2009).
54. Y. Shen and A. C. Lua, *J. Appl. Polym. Sci.*, **116**, 2906 (2010).
55. K. Balani, V. Verma, A. Agarwal and R. Narayan, in: *Biosurfaces: A materials science and engineering perspective*, K. Balani, V. Verma, A. Agarwal and R. Narayan Eds., John Wiley & Sons, Hoboken, New Jersey (2015).
56. S. S. Hosseini and S. Najari, in *Nanostructured polymer membranes, volume 2: Applications*, P. M. Visakh and N. Olga Eds., Wiley-

Scrivener, Beverly, Massachusetts (2016).
57. S. S. Hosseini, A. H. Khodakarami and E. N. Nxumalo, *Polym. Eng. Sci.*, **60**(8), 1795 (2020).
58. S. Xu and Y. Wang, *J. Membr. Sci.*, **496**, 142 (2015).
59. Y. Wang, L. Jiang, T. Matsuura, T. S. Chung and S. H. Goh, *J. Membr. Sci.*, **318**(1-2), 217 (2008).
60. W. Hao, Z. Tong, X. Liu and B. Zhang, *Sep. Purif. Technol.*, **251**, 117322 (2020).
61. A. Dobrak, A. Figoli, S. Chovau, F. Galiano, S. Simone, I. F. J. Vankelecom, E. Drioli and B. Van der Bruggen, *J. Colloid Interface Sci.*, **346**(1) 254 (2010).
62. H. Zentou, Z. Z. Abidin, R. Yunus, D. R. A. Biak and M. A. Issa, *J. Appl. Polym. Sci.*, **138**(19), 50408 (2020).
63. X. Zhan, M. Wang, T. Gao, J. Lu, Y. He and J. Li, *Sep. Purif. Technol.*, **236**, 116238 (2020).
64. L. Ye, L. Wang, X. Jie, C. Yu, G. Kang and Y. Cao, *J. Membr. Sci.*, **595**, 117540 (2020).
65. H.-A. Tsai, Y.-L. Ye, K.-R. Lee, S.-H. Huang, M.-C. Suen and J.-Y. Lai, *J. Membr. Sci.*, **368**(1-2), 254 (2011).
66. D. P. Suhas, T. M. Aminabhavi and A. V. Raghu, *Polym. Eng. Sci.*, **54**(8), 1774 (2014).
67. H. Zhang and Y. Wang, *AIChE J.*, **62**(5), 1728 (2016).
68. A. V. Penkova, M. E. Dmitrenko, N. A. Savon, A. B. Missyul, A. S. Mazur, A. I. Kuzminova, A. A. Zolotarev, V. Mikhailovskii, E. Lahderanta, D. A. Markelov, K. N. Semenov and S. S. Ermakov, *Sep. Purif. Technol.*, **204**, 1 (2018).
69. Y.-F. Lin, J.-C. Ho, K.-Y. Andrew Lin, K.-L. Tung, T.-W. Chung and C.-C. Lee, *Sep. Purif. Technol.*, **221**, 325 (2019).
70. W. Cai, X. Cheng, X. Chen, J. Li and J. Pei, *ACS Omega*, **5**(12), 6277 (2020).